View metadata, citation and similar papers at core.ac.uk
brought to you by CORE
provided by Elsevier - Publisher Connector

FEBS 29867 FEBS Letters 579 (2005) 4843–4850

Requirements of myocyte-specific enhancer factor 2A in zebrafish cardiac contractility

Yue-Xiang Wang[a], Lin-Xi Qian[a], Zhang Yu[c], Qiu Jiang[a], Yong-Xin Dong[a], Xue-Fei Liu[a], Xin-Ying Yang [a], Tao P. Zhong[a,b,*], Hou-Yan Song[a,*]

[a] *Department of Molecular Genetics, Shanghai Medical School and Key Laboratory of Molecular Medicine, Ministry of Education, Fudan University, Shanghai 200032, PR China*
[b] *Department of Medicine, Pharmacology and Cell and Developmental Biology, School of Medicine, Vanderbilt University, Nashville, TN 37232, USA*
[c] *Electron Microscope Laboratory, Shanghai Medical School, Fudan University, Shanghai 200032, PR China*

Received 29 May 2005; revised 7 July 2005; accepted 19 July 2005

Available online 9 August 2005

Edited by Angel Nebreda

Abstract Myocyte-specific enhancer factor 2A (MEF2A) regulates a broad range of fundamental cellular processes including cell division, differentiation and death. Here, we tested the hypothesis that MEF2A is required in cardiac contractility employing zebrafish as a model organism. *MEF2A* is highly expressed in heart as well as somites during zebrafish embryogenesis. Knock-down of *MEF2A* in zebrafish impaires the cardiac contractility and results in sarcomere assembly defects. Dysregulation of cardiac genes in *MEF2A* morphants suggests that sarcomere assembly disturbances account for the cardiac contractile deficiency. Our studies suggested that MEF2A is essential in cardiac contractility.
© 2005 Published by Elsevier B.V. on behalf of the Federation of European Biochemical Societies.

Keywords: MEF2A; Cardiac contractility; Zebrafish; Development; Morpholino; Morphant

1. Introduction

Heart failure is a complex disorder in which cardiac contractility is insufficient to adequately supply blood to other organs. This syndrome is a common complication that ensues from a wide variety of cardiovascular pathologies. Studies in failing human hearts show numerous morphological changes including degenerative alterations, mutation of contractile elements and marked disorganization of sarcomere. These changes suggest that defects of a contractile gene lead not only to decreased elastic properties of the sarcomere but also to disturbances in sarcomerogenesis [1–4].

The zebrafish, *Danio rerio*, offers several distinct advantages as a genetic and embryological model system, including the external fertilization, rapid development and optical clarity of its embryos. In addition, because of their small size, zebrafish embryos are not completely dependent on a functional cardiovascular system. Even in the total absence of blood circulation, they receive enough oxygen by passive diffusion to survive and continue to develop in a relatively normal fashion for several days, thereby allowing a detailed analysis of animals with severe cardiovascular defects [5–11]. By contrast, avian and mammalian embryos die rapidly in the absence of a functional cardiovascular system. Forward genetics in zebrafish has led to the identification of several mutations affecting cardiac contractility [10–13]. So far, in the large scale mutagenesis screens of zebrafish, no mutations were linked to *myocyte-specific enhancer factor 2A* (*MEF2A*) locus [8,10–14].

A loss-of-function mutation in the human *MEF2A* causes an autosomal dominant form of coronary artery disease [15,16]. These data have recently been put into question [17,18]. Deletion of *MEF2A* in mice results in sudden cardiac death as well as marked right ventricular dilation that is not explained by increased pressure of the pulmonary vasculature [19]. Despite of the sudden cardiac death phenotype, several differences exist between these mice and humans with mutations in *MEF2A*. More detailed phenotypic analysis of animals with *MEF2A* mutations will be required to uncover its biological function.

In the present study, we described that *MEF2A* is highly expressed in the heart and somites during zebrafish embryogenesis. And we provided the first evidence that MEF2A is required for zebrafish cardiac contraction. *MEF2A* knockdown results in sarcomere assembly defects, and the disturbances of sarcomere assembly could account for the cardiac contractile deficiency.

2. Materials and methods

2.1. Zebrafish embryos

Wild-type (AB* strain) zebrafish embryos were obtained from natural spawning of wild-type adults. Zebrafish were raised, maintained and staged as previously described [20,21].

2.2. RT-PCR analysis

Total RNA was extracted from different stages embryos and adult heart. RT-PCR was performed to amplify a 202 bp fragment, whose authenticity was confirmed by sequencing (*MEF2A* forward primer: ATG CCC ACT GCC TAC AAC TC, reverse primer: CAT TCT GGC TGG TGT TGA TG). Zebrafish β-actin was used as control for qualitative and quantitative assessment of the cDNA sample

*Corresponding authors. Fax: +86 21 6403 3738.
E-mail addresses: tao.zhong@vanderbilt.edu (T.P. Zhong), hysong@shmu.edu.cn (H.-Y. Song).

Abbreviations: MEF2A, myocyte-specific enhancer factor 2A; hpf, hours post fertilization; GFP, green fluorescent protein; MO, morpholino; vmhc, ventricular myosin heavy chain; amhc, atrial myosin heavy chain; cmlc2, cardiac myosin light chain 2; anf, atrial natriuretic factor; V, ventricle; A, atrium

0014-5793/$30.00 © 2005 Published by Elsevier B.V. on behalf of the Federation of European Biochemical Societies.
doi:10.1016/j.febslet.2005.07.068

(*β-actin* forward primer: TAC AGC TTC ACC ACC ACA GC, reverse primer: AAG GAA GGC TGG AAG AGA GC).The size of the *β-actin* amplicon is 206 bp.

2.3. Morpholino modified antisense oligonucleotide and microinjections

We designed one morpholino modified antisense oligonucleotide (MO, Gene Tools, LLC) against the splice donor site of *MEF2A* exon 8 to interfere with splicing (GT-MO) and another MO directed against the 5′ sequence around the putative start codon to block *MEF2A* translation (ATG-MO). The sequences for the GT-MO and ATG-MO were the 5′-GTCGTTTGTGCTCACCAGAGTTGTA-3′ and 5′-ATCTGTATCTTCTTCCGTCCCATCT-3′, respectively. A standard control MO was designed for control microinjections. The sequence for the standard control MO was 5′-CCTCTTACCT-CAGTTACAATTTATA-3′. Wild-type embryos were injected at the one-to-two cell stage with 2.5–10 ng MO per embryo.

2.4. Microinjection of the MEF2A promoter construct in zebrafish embryos

The *MEF2A*-green fluorescent protein (GFP) construct was made by linking the 1.7-kb *MEF2A* promoter with the GFP reporter gene. The construct was linearized and dissolved in 5 mM Tris–HCl, pH 8.0, 200 mM KCl, 0.05% phenol red to a final concentration of 50 ng/ml. About 3 nl of the DNA sample was microinjected into the cytoplasm of the one-to-two cell stage embryos. By using a fluorescence microscope, we observed the green fluorescence in embryos.

2.5. In situ hybridization, immunofluorescence and photography

In situ hybridization experiments with *Titin* antisense were performed as previously described [22]. Whole mount immunofluorescence experiments were performed as previously described [22], using the monoclonal antibodies MF20 and CH1, which recognizes a sarcomeric myosin heavy chain epitope and a tropomyosin epitope. MF20 and CH1 developed by Dr. Donald A. Fischman and Dr. Jim Jung-Ching Lin were obtained from the Developmental Studies Hybridoma Bank developed under the auspices of the NICHD and maintained by the University of Iowa, Department of the Biological Sciences, Iowa City IA 52242. Stained embryos were examined with Olympus BX61 and SZX12 microscopes, and photographed with a DP70 digital camera. Images were processed using Adobe Photoshop software.

2.6. Western blot

Western blot were performed as previously described [21]. The blots were incubated with the primary antibody diluted in TBST (1:200 dilution for rabbit polyclonal anti-human MEF2A antibody (C-21;Santa Cruz) and 1:500 dilution for mouse monoclonal β-actin antibody (AC-40; Sigma)). After incubating with an anti-rabbit or anti-mouse IgG-horseradish peroxidase-conjugated secondary antibody (diluted 1:1000) at room temperature for 1 h, the blots were visualized by ECL kit according to the manufacturer's instructions.

2.7. Heart rates measurement and ventricular contractility analysis

Embryos were anesthetized and transferred to a recording chamber perfused with modified Tyrode's solution (136 mM NaCl, 5.4 mM KCl, 0.3 mM NaH_2PO_4, 1.8 mM $CaCl_2$, 1 mM $MgCl_2$, 10 mM HEPES, 5 mM glucose, pH 7.3) at 48 h post fertilization (hpf). Heart rates were accounted under a dissect microscope. Cardiac contractions were recorded with a video camera (JVC, TK-C1381) as described [23]. The lengths of ventricles in diastolic and systolic conditions were measured to calculate the ventricular shortening fraction (VSF). Values are presented as mean ± S.D.

$$\mathrm{VSF} = \frac{\text{ventricular length at diastole} - \text{ventricular length at systole}}{\text{ventricular length at diastole}}.$$

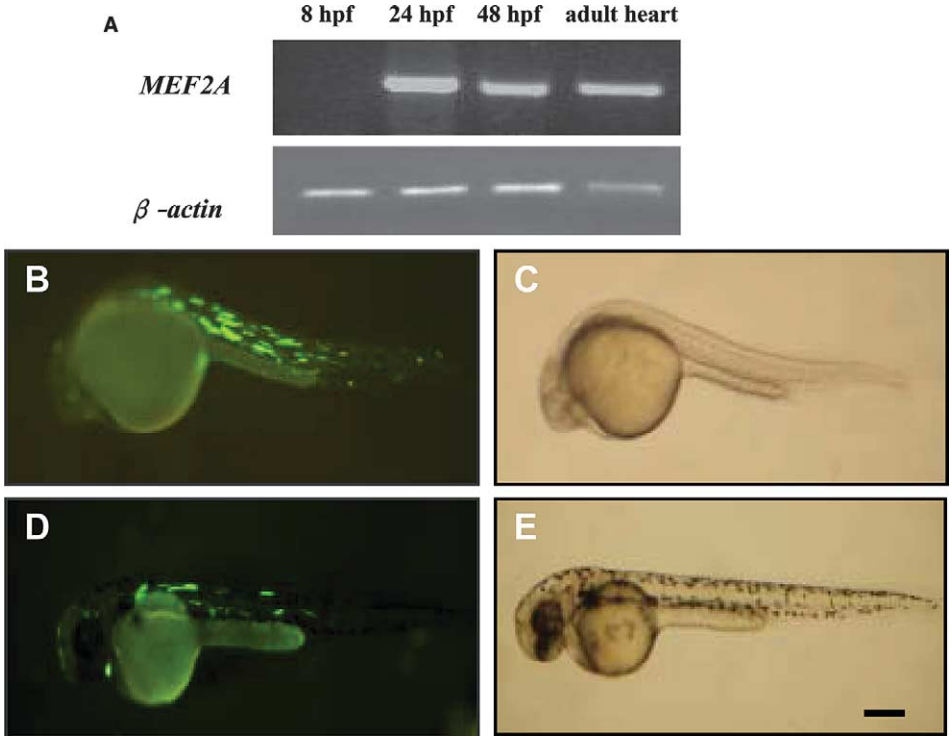

Fig. 1. *MEF2A* is highly expressed in the heart and somites during zebrafish embryogenesis. (A) RT-PCR analysis was performed with RNA samples isolated from different stages embryos and adult heart. *MEF2A* specific products were amplified from RNA isolated from 24 hpf, 48 hpf whole embryos and adult heart. The *β-actin* primers amplified a single fragment in all the samples. (B–E) Transient expression patterns of GFP fluorescence observed in *MEF2A*-promoter–GFP transgenic embryos. (B,C) Lateral views at the 24 hpf, anterior to the left. GFP expression is observed in skeletal muscle cells. (D,E) Lateral views at 48 the hpf, anterior to the left. GFP expression is observed in both heart and somites. (B,D: fluorescent field. C,E: bright field.) Scale bar, 100 μm.

2.8. Transmission electron microscopy

Embryos were fixed at 48 hpf with 2% paraformaldehyde and 2.5% glutaraldehyde in 0.1 M sodium cacodylate buffer, postfixed with 1% osmium tetraoxide followed by 1% uranyl acetate, dehydrated through a graded series of ethanol washes, and embedded in LX112 resin. Ultrathin (80 nm) sections were cut on a Reichert Ultracut UCT, stained with uranyl acetate followed by lead citrate, and viewed on a JEOL 1200EX transmission electron microscope at 80 kV.

2.9. RNA isolation and quantitative real-time PCR analysis

Total RNA was extracted from twenty microdissected hearts of 48 hpf embryos or ten 24 hpf embryos using the TRIZOL method and reverse transcribed using oligo-dT primer following the manufacturers' instructions. For all experiments, cDNA was quantified using Applied Biosystems Sequence Detection System 7300. The SYBR green method was used to quantify cDNA. The sequence-specific primers (primers sequences available on request) were designed using Primer Express2.0

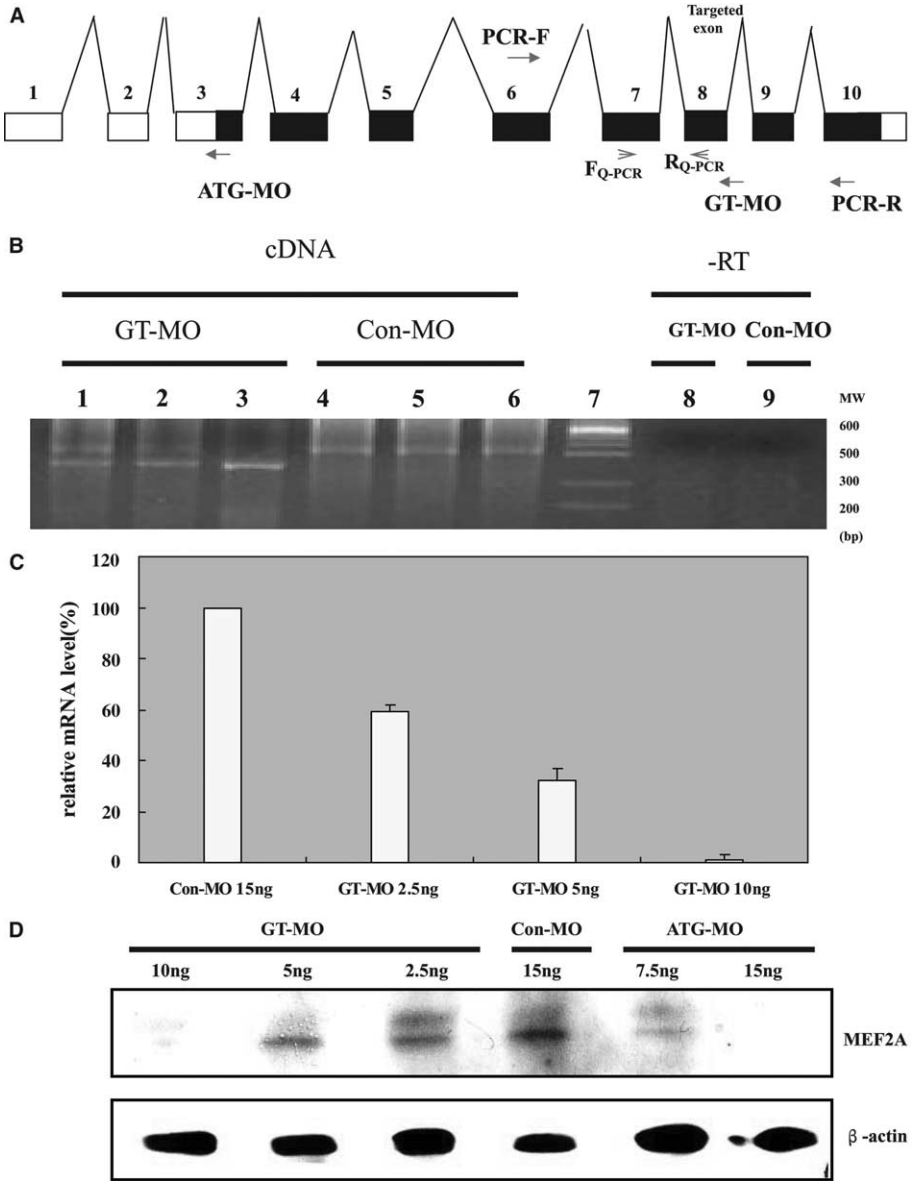

Fig. 2. Target sites of the *MEF2A* MOs and aberrant splicing of *MEF2A* transcript. (A) Genomic organization of zebrafish *MEF2A*. Arrowed lines indicate the two antisense oligos, GT-MO and ATG-MO, and the PCR primers used to detect targeted exon skipping. Forward primer (PCR-F): TCA AGG TTC AAT GCA CAG AAG CGT AGT G. Reverse primer (PCR-R): GAT GGA GAG GTT TGA GCC CTG AGG TAA GT. ATG-MO hybridizes to the start codon and is expected to block translation. GT-MO targets the splicing of the exon labeled "targeted exon". (B) Targeted exon deletion caused by the GT-MO is confirmed by RT-PCR of total RNAs isolated from 10 individual embryos injected with either GT-MO (lanes 1–3: lane 1, 2.5 ng; lane 2, 5 ng; lane 3, 10 ng) or Con-MO (lanes 4–6: lane 4, 2.5 ng; lane 5, 5 ng; lane 6, 10 ng). A 414 bp band representing the exon 8 deletion product is seen in the GT-MO injected fish only, whereas the 541 bp wild-type band is detected in both groups. Lanes 8 (pool of GT-MO samples) and 9 (pool of Con-MO samples) are no RT controls. Lane 7 is DNA ladder (bp = base pairs). PCR strategy is summarized in the diagram on (A). (C) The amount of wild-type *MEF2A* mRNA in GT-MO injected and Con-MO injected embryos were determined by quantitative real-time RT-PCR analysis. The amount of MO injected per embryo is indicated. PCR strategy is summarized in the diagram on (A). Forward primer ($F_{Q\text{-}PCR}$): CCC CCA TCC AGC AA. Reverse primer (RQ-PCR): GCT TAT CCT CTG GGT GTT C. (D) Knock-down of MEF2A protein by MO injection. Western analysis of 24 hpf-embryos injected with *MEF2A* or control MOs at the indicated doses.

Table 1
Phenotypes of wild-type embryos injected with *MEF2A* MOs

Morpholino	*n*	Phenotype			
		Normal	Downward tail curvature	Cardiac contractility defects	Downward tail curvature and cardiac contractility defects
GT-MO (10 ng)	49	1 (2%)	45 (92%)	29 (59%)	25 (51%)
ATG-MO (15 ng)	50	2 (4%)	44 (88%)	26 (52%)	23 (46%)
Con-MO (15 ng)	50	48 (96%)	1 (2%)	2 (4%)	0 (0%)

Downward tail curvature phenotype was assayed by the shape at 28 hpf. Cardiac contractility was assayed by measuring the ventricular shortening fraction at 48 hpf.

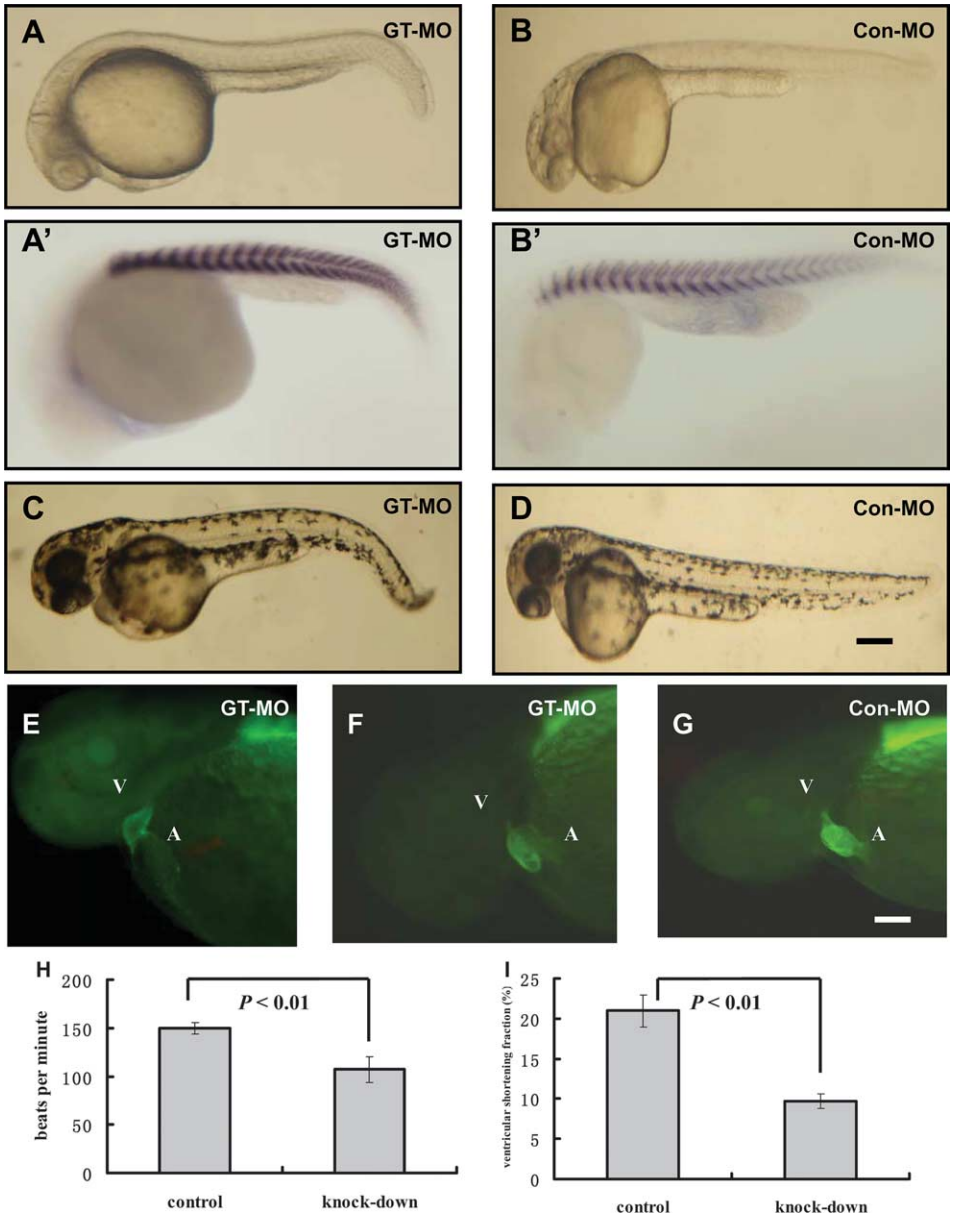

Fig. 3. Knock-down of *MEF2A* leads to cardiac contractility defects. (A–G) Lateral views with anterior to the left. (A,B) The overall morphology of a *MEF2A* GT-MO-injected (A,C) and Con-MO-injected (B,D) embryos at 28 hpf (A,B) and 48 hpf (C,D). (A′,B′) Lateral views of *titin* expression, which marks each somite border in GT-MO-injected (A′) and Con-MO-injected (B′) embryos at 28 hpf. (E-G) Whole-mount immunofluorescence with the anti-tropomyosin antibody CH1 (FITC) to show the cardiac morphology in *MEF2A* knock-down embryos. Ventricle (V) and atrium (A) are indicated. At 48 hpf, 11% ($n = 45$) of the *MEF2A* knock-down embryos show dilation of the atria and/or ventricles (E) compared with the control (G) embryos. 89% ($n = 45$) of the *MEF2A* morphants ventricles and atria are normal without obvious structural defects (F). (H,I) Comparison of the heart rate (H) and ventricular shortening fraction (I) in *MEF2A* knock-down and control embryos at 48 hpf. Scale bars: A–D, 100 μm; E–G, 50 μm.

software (Applied Biosystems, USA). No-RT controls and water controls gave similar high threshold cycle values, demonstrating that contamination contributed to less than 0.1% of quantified product. The input cDNA was normalized for PCR by using primers specific for β-actin. Data were expressed as level of expression relative to standard control-injected embryos set at 1 ± S.D. ($n = 3$).

2.10. Online supplemental material

Supplemental video material is available online. The videos show the heart beat of a *MEF2A* knock-down embryo (Movie 1) and a control embryo (Movie 2) at 48 hpf.

3. Results

3.1. MEF2A is highly expressed in zebrafish heart and somites during zebrafish embryogenesis

RT-PCR time course analysis of the zebrafish *MEF2A* expression pattern was performed with cDNA from 8, 24, 48 hpf-stage embryos and adult heart. *MEF2A* expression was detectable at 24 hpf, 48 hpf and adult heart (Fig. 1A, [24]). To better understand *MEF2A* tissue-specific expression during zebrafish embryogenesis, we isolated 5′ flanking sequences of the zebrafish *MEF2A* gene and used a GFP transgenic strategy to generate *MEF2A*-GFP transgenic zebrafish. *GFP* expression was observed in skeletal muscle cells at 24 hpf (Fig. 1B and C). At 48 hpf, *GFP* expression was observed in both heart and somites (Fig. 1D and E). The *GFP* expression pattern suggests that *MEF2A* expression is largely specific to cells of the somitic and cardiac lineages.

3.2. Effective targeted knock-down MEF2A in zebrafish

To determine the function of MEF2A in zebrafish development, we performed gene knock-down experiments using two different MO antisense oligonucleotides (GT-MO and ATG-MO) targeting the zebrafish *MEF2A* [25,26]. We designed the GT-MO directed against the donor site of exon 8 in *MEF2A*. Blocking the donor site of an exon can cause skipping of the targeted exon and/or retention of the intron [27,28]. We traced efficiency of the *MEF2A* GT-MO by RT-PCR with primers flanking the targeted exon on GT-MO-injected and standard control morpholino (Con-MO)-injected embryos at different time-points. RT-PCR on RNA from GT-MO-injected embryos at 28 hpf produced PCR products that lacked exon 8 (Fig. 2A and B). As late as 6 days post fertilization, the GT-MO modulated mRNAs were still detectable (data not shown). Sequencing of the PCR product lacking exon 8 showed that the loss of exon 8 resulted in a frameshift in the *MEF2A* mRNA and hence premature translation termination. The truncated protein would contain 3 missense amino acids and would terminate after amino acid 269. We next quantified the ability of GT-MO to reduce the amount of correctly spliced *MEF2A* mRNA by quantitative real-time RT-PCR analysis. We injected GT-MO into embryos at doses ranging from 2.5 to 10 ng MO/embryo and harvested RNA at 24 hpf. Using a SYBR green real-time RT-PCR analysis, we found that injection of GT-MO reduced the amount of wild-type *MEF2A* mRNA in a dose-dependent manner (Fig. 2C). Because injection of 10 ng GT-MO per embryo reduced the amount of wild-type message to levels that were undetectable in our assay (Fig. 2C and D), we chose this amount for all subsequent experiments involving GT-MO induced knock-down of *MEF2A*. To demonstrate that only the truncated MEF2A protein is present in 10 ng GT-MO-injected embryos, we performed western blot assay using a specific anti-human MEF2A antibody (C-21). The MEF2A antibody was raised against a peptide mapping at the carboxy terminus of MEF2A of human origin [15]. As shown in Fig. 2D, a dramatic decrease in the levels of MEF2A protein was observed after the injection of 5 ng of the GT-MO, and complete loss of detectable MEF2A protein was observed after injection of 10 ng/embryo of the same MO.

A second MO (ATG-MO) was designed against the start codon to block translation of the *MEF2A* mRNA (Fig. 2A and D) [25]. To determine the phenotype after "knock-down" of the MEF2A protein, we determined the minimum amount of the ATG-MO that could effectively block MEF2A protein synthesis in vivo. As shown in Fig. 2D, a dramatic decrease in the levels of MEF2A protein was observed after the injection of 7.5 ng of the ATG-MO, and complete loss of detectable MEF2A protein was observed after injection of 15 ng/embryo of the same MO. By contrast, the injection of 15 ng of the Con-MO had no effect on the levels of MEF2A. Thus, we injected MOs at the dosage of 15 ng/embryo to investigate the embryonic phenotype resulting from a knock-down of the MEF2A protein.

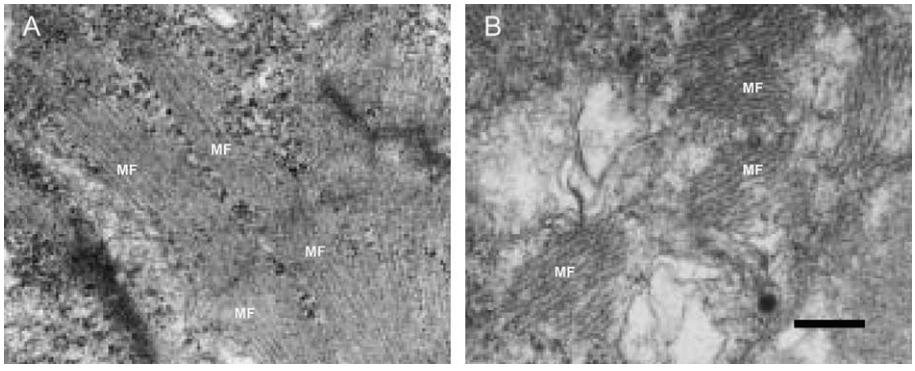

Fig. 4. Sarcomeric structures are disrupted in *MEF2A* morphants hearts. Transmission electron microscopy of zebrafish embryonic hearts at 48 hpf. Myofibrils (MF) are evident in the cardiomyocytes of both control (A) and *MEF2A* knock-down (B) embryos. The most salient differences between embryonicl cardiomyocytes from *MEF2A* morphants were the myofibrillar disorganization in the cardiac muscle. MF, myofibril. Scale bar, 300 nm.

3.3. Knock-down of MEF2A leads to cardiac contractility defects

We analyzed the phenotype in animals injected with either *MEF2A* GT-MO or ATG-MO. Phenotypes of wild-type embryos injected with *MEF2A* MOs were summarized in Table 1. In the early stages, *MEF2A* knock-down embryos display a downward tail curvature (Fig. 3A–D). *Titin* expression marks the segment borders of wild-type embryos [29]. The irregular posterior somite borders in *MEF2A* knock-down embryos (Fig. 3, compare A′ with B′) implicates that MEF2A is important in zebrafish somite development. Injection of the GT-MO or the ATG-MO caused cardiac contractility defects that are obvious in live embryos at 48 hpf (see Supplement Movie 1). A obvious characteristic blood pool caudal to the *MEF2A* morphants atria indicates that blood flow is inefficient (see Supplement Movie 1). In control embryo, the ventricle and atrium exhibit vigorous, rhythmic contractions (see supplement Movie 2). At 48 hpf, 11% ($n = 45$) of the *MEF2A* GT-MO-injected embryos show noticeable dilation of the atria and/or ventricles (Fig. 3E) compared with the Con-MO-injected embryos (Fig. 3G). The normal cardiac morphology was visible in 89% ($n = 45$) of the GT-MO-injected embryos (Fig. 3F). In control embryos, the ventricles and atria exhibit vigorous, rhythmic contractions, ensuring circulation throughout the body. At 48 hpf, control ventricles and atria contracted at 150 ± 6 beats per minute ($n = 20$), while *MEF2A* morphants ventricles and atria contracted at 107 ± 13 beats per minute ($n = 20$; $P < 0.01$; Fig. 3H). We quantified cardiac contractility by measuring the ventricular shortening fraction (VSF) [23,30]. The average VSF of the wild-type siblings is $21 \pm 2\%$ ($n = 10$), whereas the VSF value drops to $9.7 \pm 0.9\%$ in *MEF2A* morphants hearts ($n = 10$; $P < 0.01$; Fig. 3I), demonstrating that MEF2A possesses an important role in regulating cardiac contractility.

3.4. MEF2A is involved in assembly of the cardiac contractile apparatus

The functional defects in *MEF2A* morphants suggest that the cardiac contractile apparatus is abnormal. We compared sarcomere assembly in control embryos and *MEF2A* knock-down embryos at 48 hpf. At this stage, the control heart exhibits nascent sarcomeres containing both thick and thin filaments, and the nascent myofibrils assemble into higher-order sarcomere structures (Fig. 4A) [31]. By contrast, the most salient differences between embryonic cardiomyocytes from *MEF2A* knock-down embryos were the myofibrillar disorganization (Fig. 4B). These data suggest that MEF2A inhibition causes sarcomere assembly defects. The failure to generate normal sarcomeres most probably underlies the inability of the *MEF2A* morphant heart to generate significant systolic force.

3.5. Dysregulation of cardiac genes in MEF2A morphants hearts

To further investigate the molecular basis for the cardiac abnormalities in *MEF2A* morphants, we performed real-time PCR analysis of the gene expression profiles of hearts from *MEF2A* knock-down embryos and control embryos at 48 hpf. From this analysis, we detected alterations in expression of cardiac contractile apparatus genes and key transcriptional factors genes. In particular, *troponon C*, *troponon T*, *atrial myosin heavy chain* (*amhc*), *cardiac myosin light chain 2* (*cmlc2*), *α-tropmyosin* and *tbx5* were downregulated in *MEF2A* morphants hearts 0.38 ± 0.04-fold, 0.45 ± 0.02-fold, 0.18 ± 0.01-fold, 0.13 ± 0.08-fold, 0.45 ± 0.16-fold and 0.09 ± 0.10-fold, respectively. *α-Actin* and *ventricular myosin heavy chain* (*vmhc*) were only weakly downregulated 0.70 ± 0.12-fold and 0.67 ± 0.17-fold, respectively. In contrast, *MEF2D* and *nkx2.5* were upregulated 1.98 ± 0.34-fold, and 3.29 ± 0.56-fold, respectively (Fig. 5A). *MEF2D* was upregulated in *MEF2A* morphant heart, suggesting that perhaps it was compensating for the lack of *MEF2A* at this stage. Based on the results from real-time PCR analysis, which suggested that a gene program characteristic of cardiac contractility and heart failure had been dysregulated in *MEF2A* morphants hearts, we used whole mount immunofluorescence to examine the expression of genes known to be involved in cardiac contractility [1]. In agreement with the real-time PCR results, whole mount immunofluorescence showed that expression of *mhc* (Fig. 5B and C) and *α-tropmyosin* (Fig. 5D and E) was downregulated in *MEF2A* morphants hearts at 48 hpf. Together, *MEF2A* expression pattern, knock-down experiment, cardiomyocytes electron microscopy observation and the dysregulation of cardiac genes indicate that MEF2A is required in zebrafish cardiac contractility.

4. Discussion

Comparing protein sequences, zebrafish MEF2A is 72.7% identical to human MEF2A, and 63.2% identical to that of mouse, indicating that MEF2A structure is highly conserved. MEF2 was first described as a muscle-enriched transcription factor that bound to an A/T-rich DNA sequence in the control regions of numerous muscle-specific genes. MEF2 proteins are nearly identical at their N-termini; where they have a MADS domain (present in *M*CM1, *A*gamous, *D*eficiens and *S*erum response factor). This domain mediates dimerization and binding to the DNA sequence CTA(A/T)$_4$TAG/A [32]. An adjacent MEF2-specific domain influences DNA-binding affinity and cofactor interactions, and the C-terminal regions of MEF2 proteins are required for transcriptional activation [15,16,32]. The splice donor site MO directed against zebrafish *MEF2A* exon 8 can cause skipping of the targeted exon. The loss of exon 8 caused a frameshift in the *MEF2A* mRNA. This mutation that we identified is predicted to lead to a complete loss of function, as it deletes most of the DNA-binding homeodomain and the entire C-terminal portion of MEF2A.

This report has identified a novel function of *MEF2A* involved in cardiac contractility employing zebrafish as a model. In summary, a knock-down of *MEF2A* function in zebrafish impaired the cardiac contraction. *MEF2A* knock-down results in sarcomere assembly defects, and disturbances of the sarcomere assembly may account for the cardiac contractile deficiency.

The *MEF2A*-promoter–GFP transgenic zebrafish analysis and whole mount in situ hybridization experiments strongly support that *MEF2A* gene expression marks the cardiac and skeletal muscle lineages during zebrafish embryogenesis. The expression of *MEF2A* continues in adult heart. These expression patterns show that *MEF2A* is a key transcriptional factor involved in cardiomyocyte function and dysfunction.

The phenotypes of *MEF2A* morphants reveal essential roles for *MEF2A* in maintenance of cyto-architectural integrity in post-natal cardiac myocytes. Several genes involved in

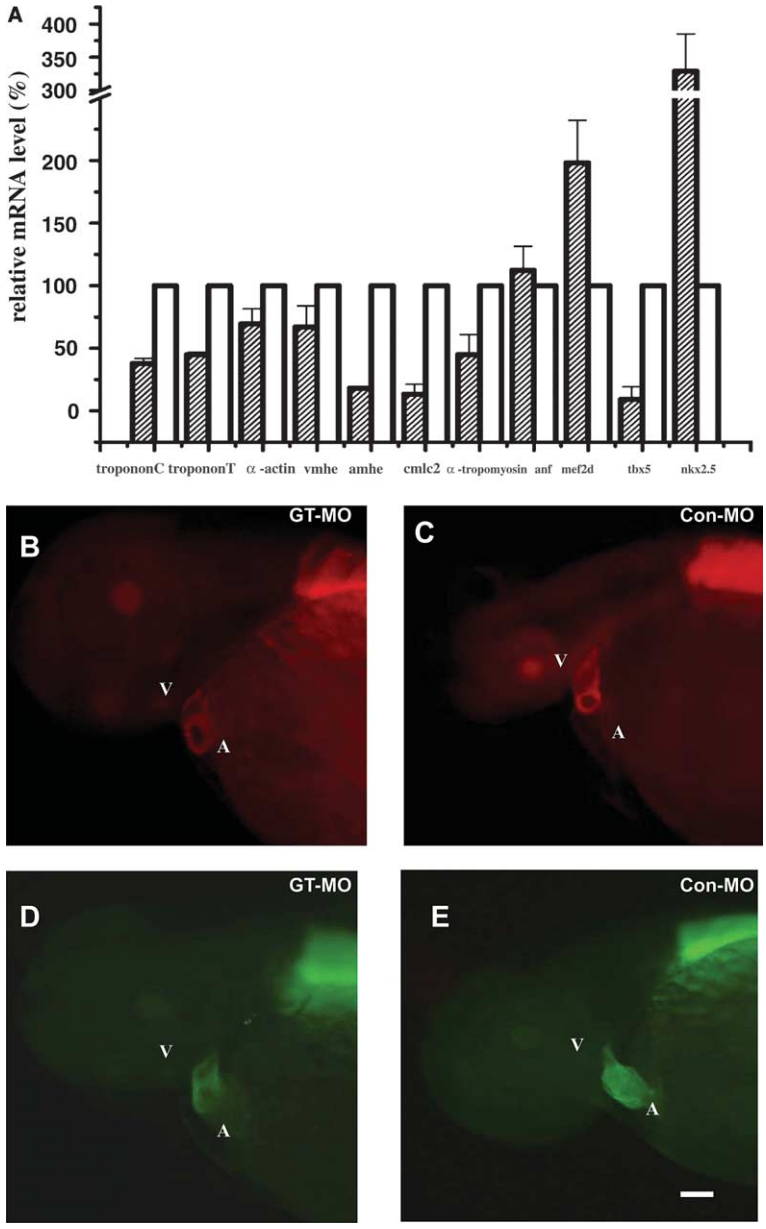

Fig. 5. Changes in gene expression in *MEF2A* morphants hearts. (A) Altered gene expression in hearts from *MEF2A* knock-down embryos compared with control embryos. (B–E) Whole-mount immunofluorescence with the monoclonal antibody MF20 (TRITC), which recognizes a sarcomeric myosin heavy chain epitope found in both the ventricle and atrium, and the anti-tropomyosin antibody CH1 (FITC) to show the downregulation of *mhc* and α-*tropmyosin*. Lateral views with anterior to the left. (B,C) Comparison of *MEF2A* knock-down (B) and control embryos (C) indicates downregulation of *mhc* expression throughout the *MEF2A* knock-down heart at 48 hpf. (D,E) Likewise, the *MEF2A* morphant heart exhibits downregulation of α-*tropmyosin* expression at this stage. Ventricle (V) and atrium (A) are indicated. Scale bar, 50 μm.

zebrafish myogenesis have promoters or enhancers that bind MEF2A (Y. Wang, T.P. Zhong and H. Song, unpublished data). Some of these genes have essential roles in sarcomerogenesis. These data may explain the cardiac contraction defects that we observed in the *MEF2A* knock-down zebrafish embryos. Studies in heart development and diseases show mutations of contractile elements give the same kind of sarcomere defects phenotypes [1–4]. The sarcomere assembly defects in *MEF2A* morphants hearts could be an indirect effect of MEF2A. It is likely that MEF2A couples with other transcription factors to regulate cardiac differentiation.

MEF2D was upregulated in *MEF2A* morphants hearts, suggesting that perhaps it was compensating for the lack of *MEF2A* at this stage. It has been reported that MEF2D can be activated by stress-responsive signaling pathways [19].*MEF2A* morphants hearts might evoke a stress response. Currently, there are four known members of the MEF2 family termed MEF2A, MEF2B, MEF2C, and MEF2D. The specific MEF2 isoform is expressed in distinct patterns and has distinct function during embryogenesis. Although *MEF2D* was upregulated in *MEF2A* morphants hearts, it cannot compensate MEF2A deficiency completely.

Our results open avenues for understanding the molecular mechanism of heart development and diseases. Investigating the multilevel controls that regulate contractile protein expression represents fascinating problems for the future.

Acknowledgements: We thank several people for their contributions to this project, particularly Lin Qi for expert technical assistance with electron microscopy, Drs. Yang Jian and Li Guoping for critical reading of the manuscript. We are also grateful to members of the Key Laboratory of Molecular Medicine for advice and support. This work was supported in part by grants from "211" major discipline project to H.-Y.S. and T.P.Z., from National Natural Science Foundation of China to T.P.Z. and H.-Y.S. (30328009), and from Fudan University Invited Professorship to T.P.Z.

Appendix A. Supplementary data

Supplementary data associated with this article can be found, in the online version, at doi:10.1016/j.febslet.2005.07.068.

References

[1] Seidman, J.G. and Seidman, C. (2001) The genetic basis for cardiomyopathy: from mutation identification to mechanistic paradigms. Cell 104, 557–567.
[2] Camici, P.G. (2004) Hibernation and heart failure. Heart 90, 141–143.
[3] Olson, T.M., Michels, V.V., Thibodeau, S.N., Tai, Y.S. and Keating, M.T. (1998) Actin mutations in dilated cardiomyopathy, a heritable form of heart failure. Science 280, 750–752.
[4] Towbin, J.A., Bowles, K.R. and Bowles, N.E. (1999) Etiologies of cardiomyopathy and heart failure. Nat. Med. 5, 266–267.
[5] Weinstein, B.M. and Fishman, M.C. (1996) Cardiovascular morphogenesis in zebrafish. Cardiovasc. Res. 31, E17–E24.
[6] Thisse, C. and Zon, L.I. (2003) Organogenesis – Heart and blood formation from the zebrafish point of view. Science 295, 457–462.
[7] Fishman, M.C. (2001) Zebrafish – The canonical vertebrate. Science 294, 1290–1291.
[8] Stainier, D.Y. (2001) Zebrafish genetics and vertebrate heart formation. Nat. Rev. Genet. 2, 39–48.
[9] Wang, Y., Zhong, T., Qian, L., Dong, Y., Jiang, Q., Tan, L. and Song, H. (2005) Wortmannin induces zebrafish cardia bifida through a mechanism independent of phosphoinositide 3-kinase and myosin light chain kinase. Biochem. Biophys. Res. Commun. 331, 303–308.
[10] Chen, J.N., Haffter, P., Odenthal, J., Vogelsang, E., Brand, M., van Eeden, F.J., Furutani-Seiki, M., Granato, M., Hammerschmidt, M., Heisenberg, C.P., Jiang, Y.J., Kane, D.A., Kelsh, R.N., Mullins, M.C. and Nusslein-Volhard, C. (1996) Mutations affecting the cardiovascular system and other internal organs in zebrafish. Development 123, 293–302.
[11] Stainier, D.Y., Fouquet, B., Chen, J.N., Warren, K.S., Weinstein, B.M., Meiler, S.E., Mohideen, M.A., Neuhauss, S.C., Solnica-Krezel, L., Schier, A.F., Zwartkruis, F., Stemple, D.L., Malicki, J., Driever, W. and Fishman, M.C. (1996) Mutations affecting the formation and function of the cardiovascular system in the zebrafish embryo. Development 123, 285–292.
[12] Berdougo, E., Coleman, H., Lee, D.H., Stainier, D.Y. and Yelon, D. (2003) Mutation of weak atrium/atrial myosin heavy chain disrupts atrial function and influences ventricular morphogenesis in zebrafish. Development 130, 6121–6129.
[13] Sehnert, A.J., Huq, A., Weinstein, B.M., Walker, C., Fishman, M. and Stainier, D.Y. (2002) Cardiac troponin T is essential in sarcomere assembly and cardiac contractility. Nat. Genet. 31, 106–110.
[14] Xu, X., Meiler, S.E., Zhong, T.P., Mohideen, M., Crossley, D.A., Burggren, W.W. and Fishman, M.C. (2002) Cardiomyopathy in zebrafish due to mutation in an alternatively spliced exon of titin. Nat. Genet. 30, 205–209.
[15] Wang, L., Fan, C., Topol, S.E., Topol, E.J. and Wang, Q. (2003) Mutation of MEF2A in an inherited disorder with features of coronary artery disease. Science 302, 1578–1581.
[16] Bhagavatula, M.R., Fan, C., Shen, G.Q., Cassano, J., Plow, E.F., Topol, E.J. and Wang, Q. (2004) Transcription factor MEF2A mutations in patients with coronary artery disease. Hum. Mol. Genet. 13, 3181–3188.
[17] Weng, L., Kavaslar, N., Ustaszewska, A., Doelle, H., Schackwitz, W., Hebert, S., Cohen, J.C., McPherson, R. and Pennacchio, L.A. (2005) Lack of MEF2A mutations in coronary artery disease. J. Clin. Invest. 115, 1016–1020.
[18] Altshuler, D. and Hirschhorn, J.N. (2005) MEF2A sequence variants and coronary artery disease: a change of heart? J. Clin. Invest. 115, 831–833.
[19] Naya, F.J., Black, B.L., Wu, H., Bassel-Duby, R., Richardson, J.A., Hill, J.A. and Olson, E.N. (2002) Mitochondrial deficiency and cardiac sudden death in mice lacking the MEF2A transcription factor. Nat. Med. 8, 1303–1309.
[20] Kimmel, C.B., Ballard, W.W., Kimmel, S.R., Ullmann, B. and Schilling, T.F. (1995) Stages of embryonic development of the zebrafish. Dev. Dyn. 203, 253–310.
[21] Westerfield, M. (2000) The Zebrafish Book, University of Oregon Press, Eugene, OR.
[22] Yelon, D., Horne, S.A. and Stainier, D.Y. (1999) Restricted expression of cardiac myosin genes reveals regulated aspects of heart tube assembly in zebrafish. Dev. Biol. 214, 23–37.
[23] Shu, X., Cheng, K., Patel, N., Chen, F., Joseph, E., Tsai, H.J. and Chen, J.N. (2003) Na,K-ATPase is essential for embryonic heart development in the zebrafish. Development 130, 6165–6173.
[24] Ticho, B.S., Stainier, D.Y., Fishman, M.C. and Breitbart, R.E. (1996) Three zebrafish MEF2 genes delineate somitic and cardiac muscle development in wild-type and mutant embryos. Mech. Dev. 59, 205–218.
[25] Nasevicius, A. and Ekker, S.C. (2000) Effective targeted gene 'knockdown' in zebrafish. Nat. Genet. 26, 216–220.
[26] Ekker, S.C. (2000) Morphant: a new systematic vertebrate functional genomics approach. Yeast 17, 302–306.
[27] Draper, B.W., Morcos, P.A. and Kimmel, C.B. (2001) Inhibition of zebrafish fgf8 pre-mRNA splicing with morpholino oligos: a quantifiable method for gene knockdown. Genesis 30, 154–156.
[28] Busch-Nentwich, E., Sollner, C., Roehl, H. and Nicolson, T. (2004) The deafness gene dfna5 is crucial for ugdh expression and HA production in the developing ear in zebrafish. Development 131, 943–951.
[29] Oates, A.C. and Ho, R.K. (2002) *Hairy/E(spl)-related* (*Her*) genes are central components of the segmentation oscillator and display redundancy with the Delta/Notch signaling pathway in the formation of anterior segmental boundaries in the zebrafish. Development 129, 2929–2946.
[30] James, P.F., Grupp, I.L., Grupp, G., Woo, A.L., Askew, G.R., Croyle, M.L., Walsh, R.A. and Lingrel, J.B. (1999) Identification of a specific role for the Na,K-ATPase alpha 2 isoform as a regulator of calcium in the heart. Mol. Cell 3, 555–563.
[31] Wanga, J., Eckberg, W.R. and Anderson, W.A. (2001) Ultrastructural differentiation of cardiomyocytes of the zebrafish during the 8–26-somite stages. J. Submicrosc. Cytol. Pathol. 33, 275–287.
[32] McKinsey, T.A., Zhang, C.L. and Olson, E.N. (2002) MEF2: a calcium-dependent regulator of cell division, differentiation and death. Trends Biochem. Sci. 27, 40–47.